

# Time-Resolved Three-Dimensional Concentration Measurements in a Gas Jet

BRANDON YIP, JOSEPH K. LAM, MICHAEL WINTER,  
MARSHALL B. LONG

Turbulence can greatly influence reaction and heat transfer rates in fluids. The topology of the three-dimensional interface between mixing fluids directly determines the location and degree of reaction. The time-resolved measurement of the three-dimensional concentration field in a transitional gas jet is reported. A thin sheet of laser light was swept through the flow volume by a rotating mirror in a time brief enough that motion of the gas was minimal. The light sheet illuminated different parallel planes within the flow, and light scattered from particles seeding the jet was imaged onto a detector. The series of two-dimensional measurements made during one scan of the flow volume constituted a full three-dimensional mapping of structures within the flow. Computer graphics software was used to reconstruct and visualize three-dimensional surfaces of constant concentration and the magnitude of the concentration gradient vector over such surfaces.

**T**URBULENCE IS A FUNDAMENTAL process in fields as diverse as combustion, meteorology, oceanography, and chemistry. Turbulence enhances fluid mixing and can therefore have a large influence on reaction and heat transfer rates (1). As fluids undergo turbulent mixing, the surface area of the interface between them increases. Time-resolved, three-dimensional measurements are required to characterize this interface. Its connectivity (2), surface-to-volume ratio (3), curvature (4), and possible fractal dimensionality (5) all require investigation. This report describes a series of experiments in which the three-dimensional structure of a nearly turbulent gas jet with high spatial and temporal resolution was successfully measured.

A description of two-dimensional laser imaging helps explain the three-dimensional technique. In planar laser imaging (6), the output of a laser is formed into a thin sheet of light with cylindrical optics and is directed through the flow field under study. The

laser sheet illuminates a planar section of the flow, and the scattered light is imaged onto a two-dimensional detector. The intensity of light scattered from any region of the illuminated slice of the flow will vary with the local temperature (7, 8), density (9-11), chemical species concentration (12), or velocity (13) by appropriate choice of the scattering mechanism whose light is detected.

Planar measurements cannot be used to study the topology of turbulent boundaries and reaction zones without some degree of ambiguity, since turbulence is a three-dimensional phenomenon. Also, vector gradients of scalar quantities can only be fully determined from three-dimensional measurements.

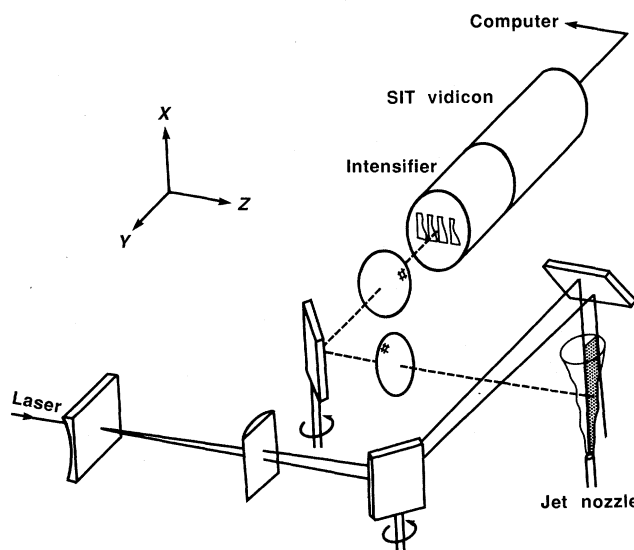
The two-dimensional optical imaging technique was extended to make three-dimensional flow measurements by rapidly scanning the laser sheet through the flow volume so that a series of parallel planes within the flow was illuminated and record-

ed. To minimize ambiguity in the measurement arising from the nonuniform velocity distribution in the flow, it was necessary that the recording time be short. To accomplish this, the laser sheet was scanned through the flow in a time brief enough that convective motion of the fluid was small—a maximum of 5% of the imaged streamwise dimension. Since a series of two-dimensional measurements had to be recorded as the laser sheet moved through the flow, extremely fast data acquisition was necessary. Earlier experiments have used reproducible flows in order to relax requirements on the data acquisition rate (14, 15). Other work has been done on three-dimensional visualization in low-speed liquid-phase flows (16). The advantages of the technique described here include its quantitative nature and its applicability to a large class of reacting and nonreacting flows, particularly higher Reynolds number gas flows.

In the first implementation of the technique, the illumination source was an argon-ion laser pulsed at 30 kHz by means of a cavity dumper (Spectra Physics models 165 and 344). During operation on all laser lines, the laser output was 0.3  $\mu$ J per 10-nsec pulse. Cylindrical lenses shaped the beam into a sheet 1 cm tall by 260  $\mu$ m thick, which was swept through a gas jet by a rotating mirror as shown in Fig. 1. The air jet was seeded with submicrometer-sized sucrose particles with an atomizing aerosol generator (Sierra Instruments model 7330). The combination of the sweep rate of the mirror (8 Hz), the separation of the mirror and the imaged region of the jet (10 cm), and the laser pulse repetition rate (30 kHz) produced a 360- $\mu$ m spacing between consecutive illuminated flow planes.

The light scattered elastically by the aerosols had an intensity directly proportional to the nozzle gas concentration (9) and was imaged onto a rectangular portion of a low-light-level camera system consisting of an image intensifier (Varo model 510-1248-309) coupled to a gated silicon-intensified-target vidicon (PARC model 1254). Data were collected on a Digital Equipment Corporation LSI 11/23 computer. Since the detector could not operate at a 30-kHz framing rate, a second rotating mirror was used to sweep six consecutive images onto different rectangular regions of the detector. Thus several slices of the flow were imaged during one sweep of the laser (that is, one slice per cavity-dumped light pulse). The information was stored on the detector as accumulated charge until all six pulses had

**Fig. 1.** Experimental arrangement used for time-resolved three-dimensional measurement of concentration in a gas jet. A cavity-dumped argon-ion laser beam was formed into a thin illumination sheet by the use of cylindrical optics and swept through an aerosol-seeded air jet with a rotating mirror. Images of parallel vertical slices of the jet were swept across a silicon-intensified target (SIT) camera with a second rotating mirror. The series of imaged planes constituted a three-dimensional recording of the flow.



Department of Mechanical Engineering and Center for Laser Diagnostics, Yale University, New Haven, CT 06520.

occurred before it was read and stored digitally on the computer, which required about 3 seconds. The data were then corrected at each image point by subtracting background counts due to digitization offsets and light scattered from the surroundings, and by normalizing to compensate for spatially nonuniform laser illumination, uneven detector sensitivity, and vignetting in the imaging optics.

In a second experiment, a faster detector was used. Again a rotating mirror (5 Hz) swept a laser sheet through the jet volume, but, instead of pulsing the laser to illuminate distinct slices of the flow and using a second rotating mirror to separate the images of the slices, these functions were performed electronically by a camera with a high framing rate. A Hadland Photonics Imacon 790 electronic framing camera was operated at a 100-kHz framing rate with a 2- $\mu$ sec exposure time per frame. The experimental arrangement was similar to that of Fig. 1, except that the second rotating mirror was

removed and the scattered light was imaged directly onto the fast camera. The argon-ion laser was operated without the cavity dumper at an output power of 4.5 W. With this arrangement 16 consecutive planes of the flow could be recorded on film during one sweep of the laser sheet through the jet volume. Since more images could be recorded with this detector, the experiment was reconfigured so that the planes were separated by only 85  $\mu$ m (the laser sheet thickness). The imaged planes were later digitized and corrected. For a flow having a calculated Reynolds number of 1100 (based on nozzle diameter), convective motion of flow structures during the 160  $\mu$ sec between the measurement of the first and last sheet corresponded to only 11 of 215 pixels in the direction of the stream.

The data were displayed by plotting surfaces where the same value was measured at all of the constituent points, similar to contour lines joining points of constant elevation on a topological map. The three-dimen-

sionality of the constant property surfaces was represented on a computer graphics monitor by means of perspective, light, shadow, and hidden surface elimination. Figure 2 shows a reconstruction of a constant concentration surface measured in the experiment. The software used was a commonly available package (MOVIE.BYU), suitably modified for our operating environment and application. Figure 3 shows the same surface color-coded by the magnitude of the concentration gradient vector, which was calculated from the three-dimensional concentration measurements (15, 17).

This representation of the data is particularly well suited for providing insight into the interaction of turbulence and combustion in turbulent reacting flows. One current model of turbulent nonpremixed combustion holds that chemical reactions take place within a thin flame sheet located wherever the stoichiometric concentrations of fuel and oxidizer exist (18). Further, the rate of heat release is proportional to the scalar dissipation rate, which can be obtained from the square of the concentration gradient magnitude. For scalar dissipation rates greater than some critical value, however, the flame is thought to extinguish. In this model of turbulent combustion, Fig. 3 can be viewed as displaying a hypothetical flame sheet with the value of the gradient indicating the amount of heat release, or, for high enough values, those regions where flame extinction is likely.

In a final experiment, the Imacon 790 camera was used again, but a different plug-in module produced a 10-MHz framing rate. To achieve adequate displacement of the laser illumination sheet in the 100-nsec interval between frames, a mirror mounted on a rapidly oscillating (2.9 kHz) resonant galvanometer positioned 1 m from the jet was used. Because of the extremely short exposure time of 20 nsec per frame, a higher power laser was required so that light scattered from the jet could be detected by the film. A flash lamp-pumped dye laser (Phase-R DL-1000 using rhodamine 590 dye) was used, and up to six parallel planes, each separated by 128  $\mu$ m were recorded within the 600-nsec duration of a single 20-mJ laser pulse. Convective motion of the fluid during the measurement interval was too small to be resolved. Unfortunately, during the time that the detector was available the optical configuration could not be optimized. As a result, the laser sheet thickness exceeded the 128- $\mu$ m spacing between imaged slices, leading to unsatisfactory resolution of structures in the flow. However, this final experiment demonstrates that recording of a three-dimensional flow field can be done during a single energetic laser pulse.



**Fig. 2.** Reconstructed constant concentration surface in the transitional region of a gas jet. The region shown is 6.8 by 2.1 by 0.7 nozzle diameters ( $d = 2$  mm) in dimension, centered at 10 diameters downstream of the nozzle orifice and with one side bisecting the upward flowing jet.

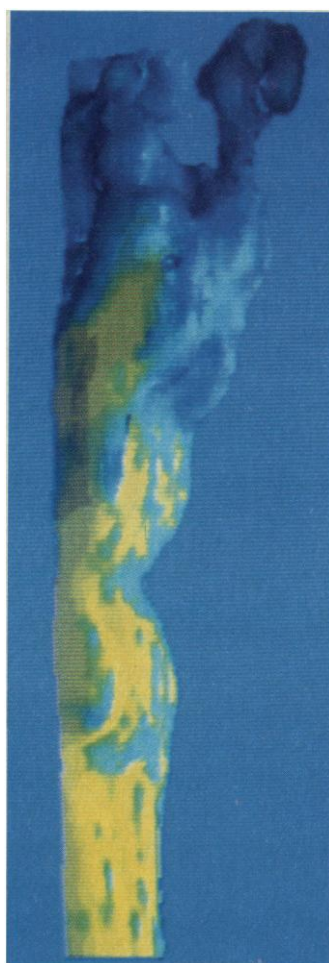


**Fig. 3.** Representation of the magnitude of the concentration gradient vector over the constant concentration surface of Fig. 2. The color assignments range from deep blue, representing the lowest gradient magnitudes, to yellow corresponding to the highest values.

## REFERENCES AND NOTES

1. P. A. Libby and F. A. Williams, Eds., *Turbulent Reacting Flows* (Springer-Verlag, New York, 1980).
2. A. R. Masri and R. W. Bilger, in *Proceedings of the 20th International Symposium on Combustion* (Combustion Institute, Pittsburgh, 1984), p. 319.
3. A. Thomas, *Combust. Flame* **65**, 291 (1986).
4. S. B. Pope, *Bull. Am. Phys. Soc.* **30**, 1694 (1985).
5. K. R. Sreenivasan and C. Meneveau, *J. Fluid Mech.* **173**, 357 (1986).
6. R. K. Hanson, in *Proceedings of the 21st International Symposium on Combustion* (Combustion Institute, Pittsburgh, 1986).
7. D. C. Fourquette, R. M. Zurn, M. B. Long, *Combust. Sci. Technol.* **44**, 307 (1985).
8. J. M. Seitzman, G. Kychakoff, R. K. Hanson, *Opt. Lett.* **10**, 439 (1985).
9. M. B. Long *et al.*, *AIJA J.* **19**, 1151 (1981).
10. A. J. R. Lysaght, R. W. Bilger, J. H. Kent, *Combust. Flame* **46**, 105 (1982).
11. M. C. Escoda and M. B. Long, *AIJA J.* **21**, 81 (1983).
12. G. Kychakoff *et al.*, *Science* **224**, 382 (1984).
13. B. Hiller and R. K. Hanson, *Opt. Lett.* **10**, 206 (1985).
14. J. C. Agui and L. Hesselink, *Bull. Am. Phys. Soc.* **30**, 1728 (1985).
15. B. Yip *et al.*, *Appl. Opt.* **25**, 3919 (1986).
16. M. K. Lynch *et al.*, *Bull. Am. Phys. Soc.* **30**, 1751 (1985).
17. B. Yip and M. B. Long, *Opt. Lett.* **11**, 64 (1986).
18. N. Peters, in *Proceedings of the 21st International Symposium on Combustion* (Combustion Institute, Pittsburgh, 1986).
19. We acknowledge the partial support of this research by the National Science Foundation (grant MSM-8351077) and the Air Force Office of Scientific Research (contract F49620-85-K-0002). We thank Hadland Photonics Ltd. for the loan of their detector.

2 September 1986; accepted 24 December 1986

## Cyclic AMP-Modulated Potassium Channels in Murine B Cells and Their Precursors

DANIEL CHOQUET, PIERRE SARTHOU, DANIELE PRIMI,  
PIERRE-ANDRÉ CAZENAVE, HENRI KORN

A voltage-dependent potassium current (the delayed rectifier) has been found in murine B cells and their precursors with the whole-cell patch-clamp technique. The type of channel involved in the generation of this current appears to be present throughout all stages of pre-B-cell differentiation, since it is detected in pre-B cell lines infected with Abelson murine leukemia virus; these cell lines represent various phases of B-cell development. Thus, the presence of this channel is not obviously correlated with B-cell differentiation. Although blocked by  $\text{Co}^{2+}$ , the channel, or channels, does not appear to be activated by  $\text{Ca}^{2+}$  entry. It is, however, inactivated by high intracellular  $\text{Ca}^{2+}$  concentrations. In addition, elevation of intracellular adenosine 3',5'-monophosphate induces at all potentials a rapid decrease in the peak potassium conductance and increased rates of activation and inactivation. Therefore, potassium channels can be physiologically modulated by second messengers in lymphocytes.

ALTHOUGH THEIR PHYSIOLOGICAL function has not been clarified, potassium channels have been detected in thymus-derived (T) cells (1-4) and their precursors (5) with the patch-clamp technique (6). These channels may play an important role in T-cell function, since the blockage of  $\text{K}^+$  currents by exogenous specific drugs results in the loss of T-cell effector functions (7). Furthermore,  $\text{K}^+$  channels can be modulated by mitogens (1, 4, 5, 8), which also regulate, in T cells, a recently described (9) inward current. None of these effects have been explained in terms of subcellular mechanisms.

In contrast, the only available data concerning ionic channels in bone marrow-derived (B) cells were obtained in hybridomas for which the presence of calcium channels was correlated with the ability to secrete immunoglobulins (Igs) (10). This scarcity of information about more usual forms of B and pre-B cells prompted us to determine the predominant type of channel in their membranes and the nature of intracellular signals influencing their behavior in order to gain clues about their possible functions.

Here we show (Fig. 1) outward voltage-dependent  $\text{K}^+$  currents in a purified murine B cell treated for 72 hours in vitro with

lipopolysaccharide (LPS), a potent activator of B lymphocytes (11). Depolarizing pulses from a holding potential of  $-80$  mV elicited an outward current detectable at  $-40$  mV, which increased in magnitude as the membrane potential was made more positive (Fig. 1A). Furthermore, as a result of prolonged depolarization this current inactivated and both activation and inactivation rates increased with increasing potential. Several observations indicate that this current is carried mainly by  $\text{K}^+$  ions. (i) When the extracellular  $\text{K}^+$  concentration was identical to that in the pipette, inward currents were elicited by voltage steps up to  $0$  mV, and above this value, outward currents were generated (Fig. 1B). (ii) Addition of tetraethylammonium chloride (TEA) ( $10$  mM) or 4-aminopyridine ( $1$  mM) to the bath blocked the channel almost completely. Furthermore, when intracellular  $\text{K}^+$  ions were replaced by  $\text{Cs}^+$  ions, no outward current was detectable. Thus, the type of  $\text{K}^+$  channels we have described here is very similar to the one previously detected in a variety of cell types, including resting and activated T cells (1-4) and more recently in T cells in an early stage of differentiation (5).

We tested whether the presence of  $\text{K}^+$  channels can be directly correlated with the degree of B-cell immunocompetency. Be-

cause the membrane of freshly collected splenocytes treated with antiserum to Thy-1 and complement (resting B cells) proved to be extremely fragile, we used cells at earlier stages of differentiation, immortalized with the Abelson murine leukemia virus (AMuLV), a retrovirus; substantial data on B-cell development have already been collected with these cells (12, 13). The ordered synthesis and expression of immunoglobulin molecules has long been used to characterize B lymphocytes at particular periods of their developmental pathway (14). Early stage pre-B cells do not produce Ig  $\mu$  heavy chain (H) or  $\kappa$  light chain (L) molecules. As differentiation proceeds, H chains accumulate in the cytoplasm before L chains. We found that all AMuLV-infected pre-B cell lines tested display  $\text{K}^+$  channels, which have properties that closely resemble those of the  $\text{K}^+$  channel found in LPS-treated lymphocytes (blasts). As above, the threshold potential for activation of the current was around  $-40$  mV in all cells studied; activation and inactivation displayed similar kinetics, although cell-to-cell variability may have prevented the detection of small differences between cell types. Along this line, the mean maximum  $\text{K}^+$  conductance, which is slightly larger in the 18-81 clone (8.5 nS; SD, 4.1 nS), than for all the other cells taken together (5.1 nS; SD, 0.67 nS;  $n = 5$ ) was the only noticeable discrepancy (Table 1). The reasons for such a discrepancy, which may be attributed to differences in cell size or in channel density, have not been investigated. However, these differences are, by far, much less than those observed in the course of T-cell cycling (4). These results suggest that the presence of  $\text{K}^+$  channels in B cells is independent of their state of immunocompetency; thus, we have selected, for most of our further studies, the 18-81 line, which is, so far, the best characterized (12, 15). In this

D. Choquet and H. Korn, Laboratoire de Neurobiologie Cellulaire, INSERM U261, Département des Biotechnologies, Institut Pasteur, 75724 Paris Cédex 15, France. P. Sarthou, D. Primi, P. A. Cazenave, Unité d'Immunochimie analytique, Département d'Immunologie, Institut Pasteur and LA CNRS 359, 75724 Paris Cédex 15, France.